Rare Metal Materials and Engineering
Volume 47, Issue 6, June 2018
Online English edition of the Chinese language journal

Available online at www.sciencedirect.com
ScienceDirect

Cite this article as: Rare Metal Materials and Engineering, 2018, 47(6): 1716-1722.

ARTICLE

Modelling Predication of Flow Stress and Grain Size in the High Temperature Deformation of Ti-6Al-2Zr-2Sn-2Mo-1.5Cr-2Nb Alloy

Luo Jiao, Gao Jun, Li Miaoquan

Northwestern Polytechnical University, Xi'an 710072, China

Abstract: A Pi-sigma fuzzy neural network (FNN), in which the layers of neural networks were organized into a feed-forward system, was used to predict the flow stress and the grain size during isothermal compression of Ti-6Al-2Zr-2Sn-2Mo-1.5Cr-2Nb alloy. After the optical micrography (OM) and scanning electron microscopy (SEM) observations, the grain size of primary α phase was measured via a quantitative metallography image analysis software. The effect of deformation temperature and strain rate on the microstructure was discussed. The comparisons of the predicted flow stress and grain size for the sample data or the non-sample data with the experimental results were given to train the models and confirm the validity in present study. The results show that the accuracy of prediction from the Pi-sigma FNN models is much high, and the Pi-sigma FNN approach can efficiently describe the non-linear and complex relationship of titanium alloys.

Key words: titanium alloys; fuzzy neural network; microstructure; flow stress; grain size

As known, it is vital to establish the constitutive equation and the microstructure model so as to optimize the processing parameters and control the microstructure of materials. Up to now, the constitutive equation and the microstructure model of materials had been developed using the empirical or semi-empirical formulas[1-3], artificial neural network (ANN)[4,5] and internal state variable (ISV) theory[6,7]. For instance, Zhang et al.[8] established the constitutive equations of 34CrNiMo steel using the working hardening curve for the working hardening and dynamic recovery period and Avrami equation for the dynamic recrystallization period. Chen et al.[9] modeled the true stress-stain responses using the Johnson Cook, modified Johnson Cook, Khan-Huang-Liang, modified Khan-Huang-Liang models. In general, these empirical or semi-empirical formulas are very simple. However, if these formulas are used beyond the experimental range for which it is designed, large calculated difference would arise, as described by Ref. [10]. In addition, these formulas can not represent the complicated and non-linear relationship between the flow stress, the microstructure and the processing parameters. To explore and understand the non-linear relationship, Lin et al.[11] established an internal-state-variable based viscoplastic constitutive equation which modeled the evolution of dislocation density, recrystallization and grain size during and after hot plastic deformation. Wang et al.[12] proposed the constitutive equations of Ti-7Mo-3Al-3Nb-3Cr alloy using dislocation density rate as an internal state variable. The physical based internal state variable approach provides the greatest potential for enhancing scientific understanding, and is especially suitable for representing the interactive relationship between the macroscopic behavior and the microstructure during the non-isothermal deformation process of materials. But, it is vital to intensively study the physical deformation mechanisms and confirm the appropriate internal state variables before establishing the internal-state-variable based constitutive equations. The ANN method does not need a mathematical formulation and has the capability of self-organization or "learning"; it is especially suitable for

Received date: June 07, 2017
Foundation item: National Natural Science Foundation of China (51575446); Natural Science Foundation of Shaanxi Province (2016JQ5070)
Corresponding author: Luo Jiao, Ph. D., Associate Professor, School of Materials Science and Engineering, Northwestern Polytechnical University, Xi'an 710072, P. R. China, Tel: 0086-29-88460328, E-mail: luojiao@nwpu.edu.cn

treating non-linear and complex relationship[13]. In present study, a fuzzy set and ANN are coupled to develop the constitutive equation and the microstructure model.

Ti-6Al-2Zr-2Sn-2Mo-1.5Cr-2Nb alloy, named as TC21 in China, is a typical two phase α+β titanium alloy. The alloy has an excellent combination of ductility, fracture toughness and strength that make it to be an ideal material in aviation industries. In the past several years, many researchers had devoted to discussing the flow behavior, the microstructure evolution and the deformation mechanisms of this alloy[14-18]. In present study, Pi-sigma fuzzy neural network (FNN), in which the layers of neural networks are organized into a feed-forward system, is used to predict the flow stress and the grain size during isothermal compression of Ti-6Al-2Zr-2Sn-2Mo-1.5Cr-2Nb alloy. The comparisons of the predicted flow stress and grain size for the sample data or the non-sample data with the experimental results are given to train the models and confirm the validity.

1 Experiment

The chemical composition of this alloy is as follows: 6.4 Al, 2.8 Mo, 2.0 Nb, 2.0 Sn, 2.2 Zr, 1.6 Cr, 0.068 Si, 0.021 Fe, 0.1 O, 0.005 C, 0.004 N and the balance Ti. The microstructure of as-received Ti-6Al-2Zr-2Sn-2Mo-1.5Cr-2Nb alloy is shown in Fig.1. It is observed that the microstructure is made of equiaxed α, lamellar α phase and a small amount of intergranular β phase. The β transus temperature of this alloy was about 1238 K[14].

Cylindrical compression specimens with a diameter of 8.0 mm and a height of 12.0 mm were cut from the Ti-6Al-2Zr-2Sn-2Mo-1.5Cr-2Nb bar. The isothermal compression was performed on a Gleeble-1500 simulator at the deformation temperatures of 1103, 1133, 1163, 1183, 1203, 1223 and 1243 K, the strain rates of 0.01, 0.1, 1.0 and 5.0 s^{-1}, and the height reductions of 50%, 60% and 70%. Prior to isothermal compression, the specimens were heated to a given temperatures at a rate of 20 K/s and held for 3 min. After isothermal compression, the specimens were cooled in air to room temperature, and were axially sectioned for the microstructure observation and the quantitative analysis. Four measurement points and four visual fields of each point in the different deformation regions were chosen. The microstructure observation was performed via a Leica DMI 3000M optical microscopy (OM). Scanning electron microscopy (SEM) were taken with a SUPRA 55 SEM operating at 15 kV. The grain size of primary α phase was measured via a quantitative metallography image analysis software (Image-Pro Plus 6.0), and was calculated by the average value of sixteen visual fields. The selected flow stress and the grain size of primary α phase are given in Table 1 and 2. It is observed that the flow stress decreases with increasing deformation temperature and decreasing strain rate; and the grain size of primary α phase is dependent on the deformation temperature, the strain rate and the strain. The detailed description of the flow behavior with processing parameters is beyond the scope of the present study, which is found in the references [14,19].

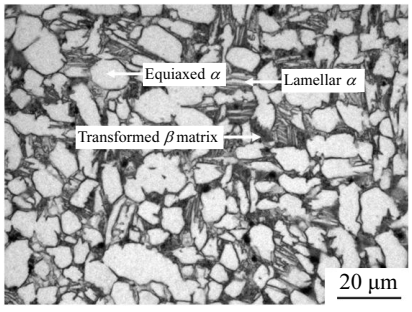

Fig.1 Optical micrograph of as-received Ti-6Al-2Zr-2Sn-2Mo-1.5Cr-2Nb alloy at room temperature

2 Microstructure Evolution

The effect of deformation temperature on the microstructure at a strain rate of 5.0 s^{-1} and a strain of 0.92 is shown in Fig.2.

Table 1 Selected flow stress of the isothermally compressed Ti-6Al-2Zr-2Sn-2Mo-1.5Cr-2Nb alloy

Strain	Strain rate/s^{-1}	Flow stress/MPa						
		1103 K	1133 K	1163 K	1183 K	1203 K	1223 K	1243 K
0.1	0.01	146.12	114.97	85.02	71.33	65.70	53.78	41.80
	0.1	211.85	180.40	134.10	100.40	92.26	81.90	68.17
	1.0	308.81	252.85	206.70	177.67	146.88	124.71	104.40
	5.0	334.46	277.39	239.42	192.79	159.37	140.05	133.03
0.2	0.01	129.69	104.45	77.87	66.29	61.52	51.22	40.04
	0.1	200.35	166.38	121.83	97.04	87.21	78.06	67.59
	1.0	297.30	241.17	196.47	169.27	140.63	122.16	102.65
	5.0	338.55	280.90	242.48	196.15	163.53	147.08	136.54
0.3	0.01	116.54	93.93	70.71	61.25	58.06	48.67	37.71
	0.1	182.28	150.02	110.58	86.96	81.66	72.95	65.84
	1.0	282.51	229.48	188.29	160.87	135.77	118.96	99.73
	5.0	315.27	263.37	230.21	186.91	155.90	143.88	135.37
0.4	0.01	105.04	85.75	64.57	57.05	53.90	45.47	36.04
	0.1	169.13	137.17	102.40	81.08	77.49	68.48	62.92
	1.0	266.08	216.63	180.11	153.31	130.22	114.49	96.22
	5.0	304.32	257.53	224.08	181.03	152.43	139.41	131.87
0.5	0.01	96.83	78.74	60.48	53.59	49.74	42.28	34.29
	0.1	157.63	126.65	95.25	76.04	73.33	65.28	60.58
	1.0	252.94	206.11	173.98	146.59	125.37	110.65	93.89
	5.0	274.19	234.16	207.72	170.95	143.41	133.66	127.78
0.6	0.01	93.54	74.07	57.42	50.33	48.35	39.72	33.12
	0.1	147.77	118.47	90.13	71.00	69.17	62.09	58.25
	1.0	241.43	197.93	169.89	142.39	121.90	108.10	92.72
	5.0	260.49	225.98	201.58	165.07	139.94	129.82	125.44
0.7	0.01	86.97	70.56	58.44	48.65	46.97	39.13	34.88
	0.1	139.55	111.46	84	65.96	67.78	60.22	57.07
	1.0	233.22	192.09	165.80	138.19	117.74	105.59	93.30
	5.0	241.33	210.79	190.34	157.51	133.69	126.04	123.69

Table 2 Comparison of the predicted with the experimental grain size of primary α phase for the partial sampled data

Deformation temperature/K	Strain rate/s^{-1}	Strain	Grain size /μm		Error/%
			Experimental	Calculated	
1103	5.0	0.92	8.15	8.33	2.25
	1.0	0.92	8.47	8.44	–0.35
	0.1	0.92	8.39	8.35	–0.47
	0.01	0.92	9.32	9.36	0.42
1133	1.0	0.69	8.10	8.09	–0.11
	1.0	1.20	7.94	7.93	–0.06
	0.01	1.20	8.67	8.68	0.07
1133	5.0	0.92	8.60	8.48	–1.43
	1.0	0.92	8.55	8.57	0.30
	0.1	0.92	8.27	8.34	0.94
	0.01	0.92	9.38	9.37	–0.08
1183	5.0	0.92	7.62	7.71	1.23
	1.0	0.92	7.14	7.52	5.40
	0.1	0.92	7.36	7.22	–1.86
	0.01	0.92	7.27	7.33	0.83

From Fig.2, it is observed that the volume fraction of primary α phase decreases significantly with increasing deformation temperature because of the phase transformation from α to β. At 1103 K (Fig.2a), equiaxed primary α phases with a size of about 8.15 μm and a small amount of elongated α phase are observed. When the deformation temperature is 1163 K, the grain size of equiaxed primary α phase becomes to be about 7.20 μm, and the microstructure has a slight oriented characteristic (Fig.2b). When the deformation temperature is in the range of 1183~1203 K, the grain size of primary α phase decreases from 7.62 μm to 7.40 μm (Fig.2c and 2d). According to above-mentioned analysis, it is seen that the variation of grain size of primary α phase with deformation temperature is oscillatory. The main reason is attributed to two aspects. Firstly, the grain growth will occur as the deformation temperature increases. Secondly, the phase transformation from α to β will lead to the decrease of grain size. Thus, the combined effect of the two aspects will finally result in the oscillatory variation of grain size.

Fig.3 shows the effect of strain rate on the microstructure at a deformation temperature of 1133 K and a strain of 0.92. It is seen in Fig.3 that the strain rate has some effect on the morphology and the grain size of primary α phase. At 0.01 s^{-1}, the microstructure is uniform and the grain size of primary α phase is about 9.38 μm (Fig.3a). When the strain rate is up to 5.0 s^{-1}, the microstructure has an oriented characteristic (Fig.3b), and is non-uniform with a mixed structure of equiaxed and elongated primary α phase. The grain size of primary α phase is about 8.60 μm. The main reason is that lower strain rate provides enough time for the grain growth and the globularization of primary α phase.

3 Constitutive Equation and Microstructure Model Using FNN

In present study, a Pi-sigma FNN is used to predict the flow stress and the grain size during isothermal compression of Ti-6Al-2Zr-2Sn-2Mo-1.5Cr-2Nb alloy, and its characteristic is described as follows: (1) the activation function of the fuzzy subset will be revised during the training of the network; (2) the fuzzy predictive model will be automatically updated in a supervised manner.

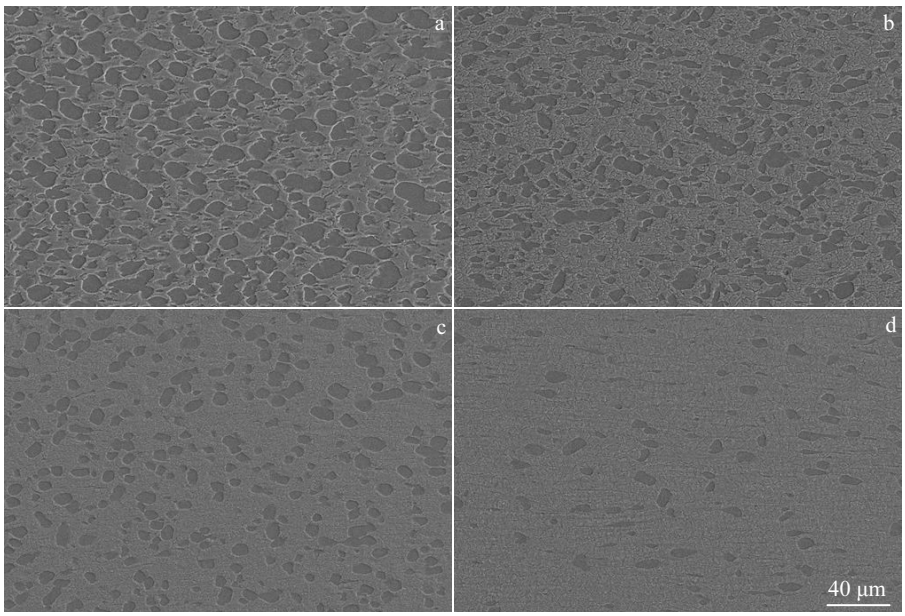

Fig.2 SEM microstructures of samples at different deformation temperatures, a strain rate of 5.0 s^{-1} and a strain of 0.92: (a) 1103 K, (b) 1163 K, (c) 1183 K, and (d) 1203 K

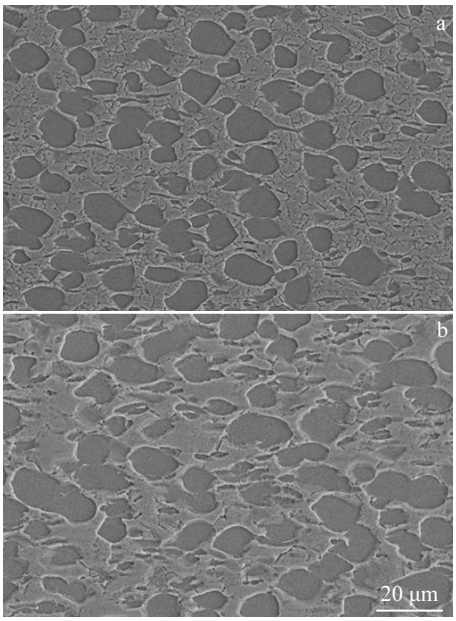

Fig.3 SEM microstructure of samples at a deformation temperature of 1133 K and a strain of 0.92 and strain rate of 0.01 s^{-1} (a), 5.0 s^{-1} (b)

The layers of neural networks in Pi-sigma FNN model are organized into a feed-forward system, and are shown in Fig.4[13]. It is observed in Fig.4 that the input variables of the network $x_1,\cdots,x_n$ are regarded as the deformation temperature, strain rate and strain, and so on. $p_0^i,\cdots p_n^i$ are the weight coefficients in the hidden layer of the network. y^i is the output in the hidden layer of the network. S and P are the addition and multiplication operations, respectively. Y is the final output of the network denoted as the flow stress or the grain size.

The neural networks have six layers and are represented as follows:

(1) Layer 1: layer 1 is the input layer of the networks; its function is to transmit the input variables (deformation temperature, strain rate and strain, and so on) into the next layer.

(2) Layer 2: the fuzzy subset of input variables with large $\{UL\}$, middle $\{UM\}$ and small $\{US\}$ is regulated in this layer, and the activation function with sigmoid shape is given as follows:

$$\mu_j^i = \exp[-(x_j - a_j^i)^2 / b_j^i] \quad (1)$$

where a_j^i and b_j^i are the constants.

(3) Layer 3: layer 3 is the fuzzy rule layer. The total of fuzzy rules can be represented as:

According to the fuzzy rule R^1:

If x_1 is UL, x_2 is UL, …, x_n is UL

Then $y^1 = p_0^1 + p_1^1 x_1 + p_2^1 x_2 + \cdots + p_n^1 x_n \quad (2)$

$$w^1 = \mu_1^1 \cdot \mu_2^1 \cdots \mu_n^1 \quad (3)$$

.

.

.

And for the fuzzy rule R^m:

If x_1 is US, x_2 is US, …, x_n is US

Then $y^m = p_0^m + p_1^m x_1 + p_2^m x_2 + \cdots + p_n^m x_n \quad (4)$

$$w^m = \mu_1^m \cdot \mu_2^m \cdots \mu_n^m \quad (5)$$

where m is the number of the fuzzy rule. According to the fuzzy subset, m is equal to 3^n; n is the number of the input variables. In present study, it is equal to 3 (deformation temperature, strain rate and strain).

(4) Layer 4: the multiplication operation is carried out in this layer, so the output $y^{(4\text{th})}$ of the layer is given by:

$$y^{(4\text{th})} = \mu_1^i(x_1)\cdot\mu_2^i(x_2)\cdots\mu_n^i(x_n)\cdot(p_0^i + p_1^i x_1 + \cdots + p_n^i x_n) \quad (6)$$

(5) Layer 5: the addition operation is carried out in this layer, so the output $y^{(5\text{th})}$ of the layer is given by:

$$y^{(5\text{th})} = \sum_{i=1}^{m}[\mu_1^i(x_1)\cdot\mu_2^i(x_2)\cdots\mu_n^i(x_n)\cdot(p_0^i + p_1^i x_1 + \cdots + p_n^i x_n)] \quad (7)$$

(6) Layer 6: the total output (y) is the following equation:

$$Y = \sum_{i=1}^{m} w^i y^i \Big/ \sum_{i=1}^{m} w^i = \frac{\sum_{i=1}^{m}[\mu_1^i(x_1)\cdot\mu_2^i(x_2)\cdots\mu_n^i(x_n)\cdot(p_0^i + p_1^i x_1 + \cdots + p_n^i x_n)]}{\sum_{i=1}^{m}[\mu_1^i(x_1)\cdot\mu_2^i(x_2)\cdots\mu_n^i(x_n)]} \quad (8)$$

Moreover, an error back-propagation (BP) algorithm with a gradient search technique is used to train the network. The average squared error is given in the following equation:

$$E = \frac{1}{2}(y_d - Y)^2 \quad (9)$$

where y_d is the experimental results.

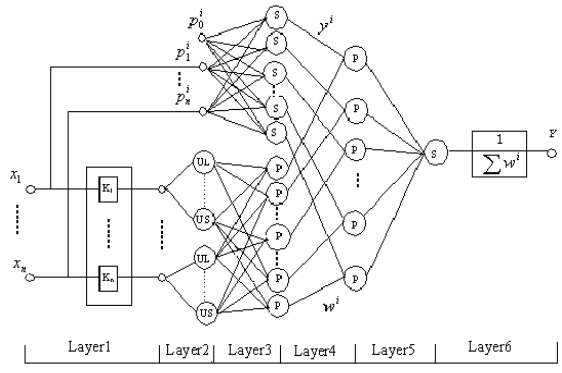

Fig.4 Layers of neural networks[13]

3.1 Constitutive equation

Three inputs of the network, including deformation temperature (T/K), strain rate ($\ln(\dot{\varepsilon}/s^{-1})$) and strain ($\varepsilon$), are represented as x_1, x_2 and x_3, respectively. The fuzzy subset of three inputs with large $\{UL\}$, middle $\{UM\}$ and small $\{US\}$ is shown in Fig.5. The subject functions are described as follows:

For the deformation temperature in Fig.5a:

$$UL_1(x) = \begin{cases} 1 & \cdots\cdots x \geq 1243 \\ \exp\left[\dfrac{-(x-1243)^2}{2200}\right] & \cdots\cdots x < 1243 \end{cases} \quad (10)$$

$$UM_1(x)=\exp\left[\frac{-(x-1173)^2}{1300}\right] \tag{11}$$

$$US_1(x)=\begin{cases}1 & \cdots\cdots x\le 1103\\ \exp\left[\dfrac{-(x-1103)^2}{2200}\right] & \cdots\cdots x>1103\end{cases} \tag{12}$$

For the strain rate in Fig.5b:

$$UL_2(x)=\begin{cases}1 & \cdots\cdots x\ge 1.60\\ \exp\left[\dfrac{-(x-1.60)^2}{20}\right] & \cdots\cdots x<1.60\end{cases} \tag{13}$$

$$UM_2(x)=\exp\left[\frac{-(x+1.50)^2}{7}\right] \tag{14}$$

$$US_2(x)=\begin{cases}1 & \cdots\cdots x\le -4.60\\ \exp\left[\dfrac{-(x+4.60)^2}{20}\right] & \cdots\cdots x>-4.60\end{cases} \tag{15}$$

For the strainin Fig. 5c

$$UL_3(x)=\begin{cases}1 & \cdots\cdots x\ge 0.85\\ \exp\left[\dfrac{-(x-0.85)^2}{0.03}\right] & \cdots\cdots x<0.85\end{cases} \tag{16}$$

$$UM_3(x)=\exp\left[\frac{-(x-0.45)^2}{0.035}\right] \tag{17}$$

$$US_3(x)=\begin{cases}1 & \cdots\cdots x\le 0.05\\ \exp\left[\dfrac{-(x-0.05)^2}{0.03}\right] & \cdots\cdots x>0.05\end{cases} \tag{18}$$

In the study, the flow stresses of 340 groups as the sample data are selected to train the FNN model. Moreover, the flow stresses of 64 groups as the non-sample data are used to confirm the validity of the model. As a result, the comparisons between the predicted and the experimental flow stress for the sampled and non-sampled data are shown in Fig.6 and Fig.7, respectively. It is seen in Fig.6 that the maximum difference and the minimum difference between the predicted and the experimental flow stress for the sample data are 11.35% and 0.01%, respectively. From Fig.7, it is seen that the maximum difference and the minimum difference between the predicted and the experimental flow stress for the non-sample data are 13.66% and 0.12%, respectively. So, the FNN model can efficiently predict the deformation behavior during isothermal compression of Ti-6Al-2Zr-2Sn-2Mo-1.5Cr-2Nb alloy.

3.2 Microstructure model

In the microstructure model, the fuzzy subset of three inputs with large {*UL*}, middle {*UM*} and small {*US*} is shown in Fig.8. The subject functions are described as follows:

For the deformation temperature in Fig.8a:

$$UL_1(x)=\begin{cases}1 & \cdots\cdots x\ge 1203\\ \exp\left[\dfrac{-(x-1203)^2}{1900}\right] & \cdots\cdots x<1203\end{cases} \tag{19}$$

$$UM_1(x)=\exp\left[\frac{-(x-1153)^2}{1300}\right] \tag{20}$$

$$US_1(x)=\begin{cases}1 & \cdots\cdots x\le 1103\\ \exp\left[\dfrac{-(x-1103)^2}{1900}\right] & \cdots\cdots x>1103\end{cases} \tag{21}$$

For the strain rate in Fig.8b:

$$UL_2(x)=\begin{cases}1 & \cdots\cdots x\ge 1.60\\ \exp\left[\dfrac{-(x-1.60)^2}{20}\right] & \cdots\cdots x<1.60\end{cases} \tag{22}$$

$$UM_2(x)=\exp\left[\frac{-(x+1.50)^2}{3}\right] \tag{23}$$

$$US_2(x)=\begin{cases}1 & \cdots\cdots x\le -4.60\\ \exp\left[\dfrac{-(x+4.60)^2}{20}\right] & \cdots\cdots x>-4.60\end{cases} \tag{24}$$

For the strainin Fig. 8c

$$UL_3(x)=\begin{cases}1 & \cdots\cdots x\ge 1.20\\ \exp\left[\dfrac{-(x-1.20)^2}{0.02}\right] & \cdots\cdots x<1.20\end{cases} \tag{25}$$

$$UM_3(x)=\exp\left[\frac{-(x-0.95)^2}{0.04}\right] \tag{26}$$

$$US_3(x)=\begin{cases}1 & \cdots\cdots x\le 0.69\\ \exp\left[\dfrac{-(x-0.69)^2}{0.02}\right] & \cdots\cdots x>0.69\end{cases} \tag{27}$$

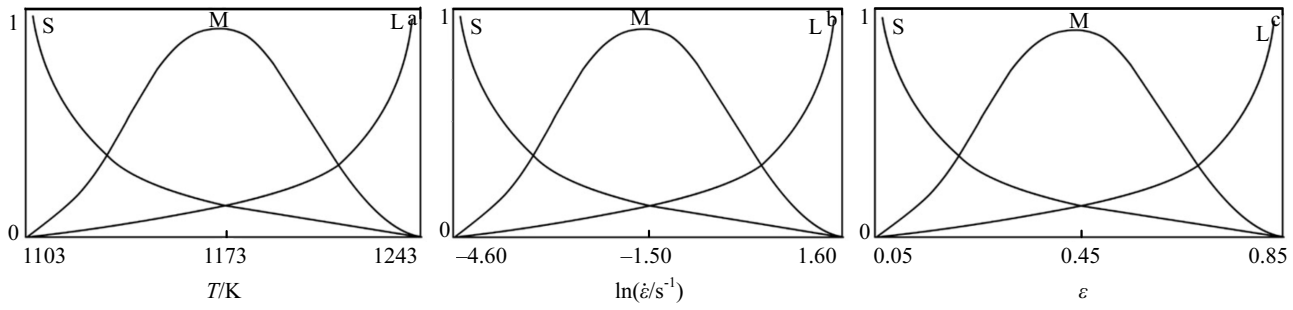

Fig.5 Fuzzy subsets for constitutive equation: (a) deformation temperature, (b) strain rate, and (c) strain

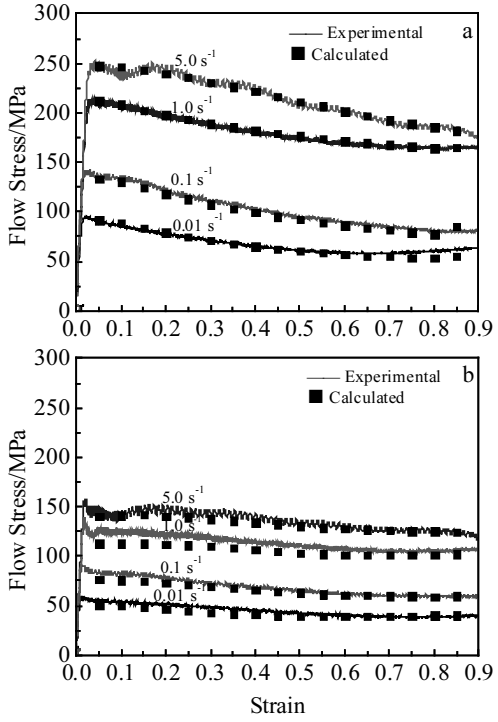

Fig.6 Comparison between the predicted and the experimental flow stress for the sampled data: (a) 1163 K and (b) 1223 K

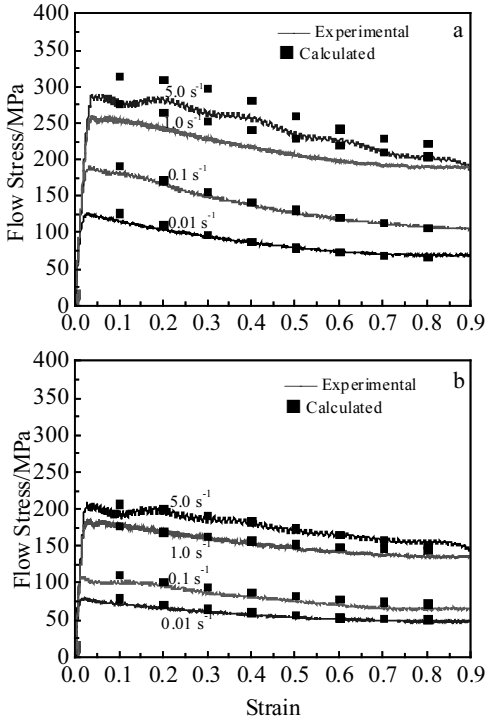

Fig.7 Comparison between the predicted and the experimental flow stress for the non-sampled data: (a) 1133 K and (b) 1183 K

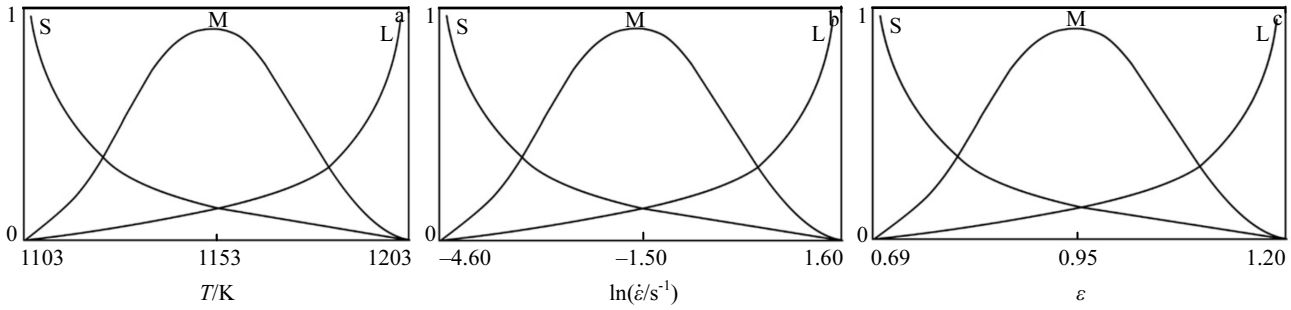

Fig.8 Fuzzy subsets for microstructure model: (a) deformation temperature, (b) strain rate and (c) strain

The grain sizes of 54 groups as the sample data are selected to train the FNN model. Moreover, the grain sizes of 6 groups as the non-sample data are used to confirm the validity of the microstructure model. Finally, the comparison between the predicted and the experimental grain size for the partial sampled data is shown in Table 2. It is seen in Table 2 that the maximum difference and the minimum difference between the predicted and the experimental grain size for the sample data are 5.40% and –0.06%, respectively. Table 3 shows the comparison between the predicted and the experimental grain size for the non-sampled data. It is seen that the maximum difference and the minimum difference between the predicted and the experimental grain size for the non-sample data are –13.99% and –0.68%, respectively.

Table 3 Comparison of the predicted with the experimental grain size of primary *α* phase for non-sampled data

Deformation temperature/K	Strain rate/s^{-1}	Strain	Grain size/μm		Error/%
			Experimental	Calculated	
1133	0.1	0.69	9.41	8.75	–6.94
1133	0.01	1.20	9.12	8.39	–8.03
1163	5.0	0.92	7.20	7.94	10.33
1163	1.0	0.92	8.11	8.05	–0.68
1163	0.1	0.92	9.05	7.78	–13.99
1163	0.01	0.92	8.79	8.01	–8.92

4 Conclusions

1) A Pi-sigma FNN model combining the fuzzy logicality with neural network technology can be used to predict the flow stress and the grain size during isothermal compression of Ti-6Al-2Zr-2Sn-2Mo-1.5Cr-2Nb alloy.

2) The comparisons between the predicted and the experimental results show that the accuracy of prediction from the Pi-sigma FNN model is much high, and the Pi-sigma FNN approach can efficiently describe the non-linear and complex relationship of titanium alloys.

References

1 Zhan H Y, Wang G, Kent D *et al*. *Materials Science and Engineering A*[J], 2014, 612: 71

2 Ghavam M H, Morakabati M, Abbasi S M *et al*. *Transactions of Nonferrous Metals Society of China*[J], 2015, 25(3): 748

3 Liu Y G, Liu J, Li M Q *et al*. *Computational Materials Science*[J], 2014, 84: 115

4 Peng W W, Zeng W D, Wang Q J *et al*. *Materials and Design*[J], 2013, 51: 95

5 Zhao J W, Ding H, Zhao W J *et al*. *Computational Materials Science*[J], 2014, 92: 47

6 Tan K, Li J, Guan Z J *et al*. *Materials and Design*[J], 2015, 84: 204

7 Fan X G, Yang H. *International Journal of Plasticity*[J], 2011, 27: 1833

8 Zhang C, Zhang L W, Shen W F *et al*. *Materials and Design*[J], 2016, 90: 804

9 Chen G, Ren C Z, Qin X D *et al*. *Materials and Design*[J], 2015, 83: 598

10 Sun Z C, Yang H, Han G J *et al*. *Materials Science and Engineering A*[J], 2010, 527: 3464

11 Lin J, Liu Y, Farrugia D C J *et al*. *Philosophical Magazine*[J], 2005, 85(18): 1967

12 Wang Y H, Han F B, Kou H C *et al*. *Rare Metal Materials and Engineering*[J], 2015, 44(8): 1883

13 Luo J, Li M Q, Hu Y Q *et al*. *Materials Characterization*[J], 2008, 59: 1386

14 Luo J, Gao J, Li L *et al*. *Journal of Alloys and Compounds*[J], 2016, 667: 44

15 Zhu Y C, Zeng W D, Liu J L *et al*. *Materials and Design*[J], 2012, 33: 264

16 Fei Y H, Zhou L, Qu H L *et al*. *Materials Science and Engineering A*[J], 2008, 494: 166

17 Jia Z Q, Zeng W D, Zhang Y W *et al*. *Journal of Alloys and Compounds*[J], 2015, 640: 488

18 Zong Y Y, Liang Y C, Yin Z W *et al*. *International Journal of Hydrogen Energy*[J], 2012, 37: 13 631

19 Gao J, Li M Q, Li X D *et al*. *Rare Metals*[J], 2015, 34(9): 625

高温变形过程中 Ti-6Al-2Zr-2Sn-2Mo-1.5Cr-2Nb 合金的流动应力和晶粒尺寸的模型预测

罗　皎，高　峻，李淼泉

(西北工业大学，陕西 西安 710072)

摘　要：采用前向型模糊神经网络模型预测 Ti-6Al-2Zr-2Sn-2Mo-1.5Cr-2Nb 合金等温压缩过程中的流动应力和晶粒尺寸。金相和 SEM 观察后，采用定量分析软件测量初生 α 相晶粒尺寸，并且研究了变形温度和应变速率对微观组织的影响。部分流动应力和晶粒尺寸作为样本数据用于训练模型，另一部分流动应力和晶粒尺寸作为非样本数据用于测试模型的可靠性。结果表明：模型的预测精度较高，该模型较好地描述了钛合金在高温变形过程中的流动行为和微观组织演变。

关键词：钛合金；模糊神经网络；微观组织；流动应力；晶粒尺寸

作者简介：罗　皎，女，1981 年生，博士，副教授，西北工业大学材料学院，陕西 西安 710072，电话：029-88460465，E-mail: luojiao@nwpu.edu.cn